STRENGTHENING OF PRESTRESSED SPUN CONCRETE POLES USING CFRP WRAPPING

Fouad H. Fouad, PhD, PE, Professor and Chair, Dept. of Civil, Construction, and Environmental Engineering, University of Alabama at Birmingham, Birmingham, AL
Ashraf M. Shalaby, PhD, PE, Research Scientist, Dept. of Civil Engineering, National Research Center, Egypt
Ronald Albanese, MSCE, PE, Senior Engineer, Valmont-Newmark**,** Birmingham, AL

ABSTRACT

Prestressed spun concrete poles are lifeline structures primarily used for supporting electric power transmission lines, which are part of our critical infrastructure. Despite the resilience of these structures, they can be damaged due to a variety of reasons, such as natural disasters (extreme wind and storm surges), accidents in the field, and vehicle collision. A reliable and rapid repair method is needed to restore the structural integrity of the poles and maintain electric power.

In certain situations, strengthening of the precast concrete poles may be needed, which is a more cost-effective solution than replacement of the entire structure. Advanced materials for strengthening and repair are becoming more commonly available as the infrastructure ages and replacement costs increase.

This paper presents the results of an experimental study conducted to evaluate the strengthening of prestressed spun concrete poles using carbon fiber reinforced polymer (CFRP) wrapping technique. Two prototype pole specimens were manufactured under normal precast concrete plant conditions. The poles were wrapped using two different wrapping schemes and were tested under four point loading in the laboratory. The results of show that CFRP wrapping can: 1) restore the original capacity of the damaged cross section; and 2) add significant strength to the cross section, over and beyond the original ultimate strength of the member.

Keywords: Concrete Poles, Carbon Fiber Reinforced Polymers, FRP, Repair, Strengthening

INTRODUCTION

Prestressed spun concrete poles are used primarily for supporting electric power transmission lines and for area lighting. They can be damaged due to natural disasters, such as extreme wind and storm surges, or due to human disasters, such as vehicle collisions. This damage significantly impacts the public, businesses, and the economy and requires replacement or repair of the poles to restore their structural integrity. In addition, the rapid development of society often renders these poles unable to sustain the increased demands placed on them, thus requiring strengthening or replacement.

With environmental and economic aspects in mind, it is untenable to replace all structures. As new materials and upgrading methods are being developed, strengthening and repairing are becoming more common than replacing the structure. One of the new advanced materials used in strengthening and repairing is fiber reinforced polymers (FRP).

FRP are showing an immense potential as a construction material and are gaining wide acceptance because of their unique characteristics. FRP have a high strength-to-weight and stiffness-to-weight ratios, adaptable performance through anisotropy, light weight, corrosion resistance, and potentially high environmental durability. FRP have been used as an externally bonded system for strengthening of concrete structures[1-4] and as a reinforcement for structural concrete elements.[5-8]

Wrapping of structural elements is a strengthening technique where a material, strong in tension and relatively stiff, is bonded around the circumference of the structural element, providing confinement in one direction and increasing the stiffness and strength in the perpendicular direction. Wrapping of reinforced concrete members subjected to compression using FRP had been successful.[9-11] Carbon fiber reinforced polymer (CFRP) has demonstrated exceptional properties as a wrapping material to provide confinement and strengthening.[2,12,13] Epoxy resin is used to bond the CFRP wrapping to the structural element.

A major advantage of CFRP as a strengthening material is its adaptability to various geometrical shapes. It can also be applied to a structure already in service, which eliminates any downtime. Furthermore, CFRP strengthening does not require special equipment or highly skilled labor for its application.

This paper presents the results of an experimental program that was conducted at the University of Alabama at Birmingham to study the strengthening of prestressed spun concrete poles using CFRP wrapping technique.

EXPERIMENTAL PROGRAM

The main objective of the experimental program was to evaluate the strengthening of prestressed spun concrete poles using CFRP wrapping. Two prototype pole specimens were manufactured under normal precast concrete plant conditions. The poles were 20 ft long

(6096 mm) with 1.5% (0.18 in/ft) conicity. The poles were wrapped using two different wrapping schemes and were tested under four point loading.

MATERIAL PROPERTIES

The prestressed spun concrete test poles were produced of a high-strength concrete mix at the Valmont spun concrete pole manufacturing facility in Alabama. The 28-day compressive strength of the concrete was 11,000 psi (75.84 MPa). Seven wire, ½" (13 mm) diameter, prestressing strand per ASTM A41614 were used. The nominal ultimate strength of the prestressing strand was 270 ksi (1860 MPa). Steel wire 3/16" (5.00 mm) in diameter per ASTM A8215 was used as spiral for the transverse reinforcement. The CFRP is a high strength, unidirectional carbon fiber fabric. The properties of the CFRP wrapping as provided by the manufacture are given in Table 1.

Table 1. Typical properties of CFRP wrapping

Ply thickness (in)	Tensile Strength (ksi)	Tensile Modulus (ksi)	Elongation (%)
0.04	104.00	9446.6	0.98

Note: 1in = 25.4 mm 1 ksi = 6.89 MPa

SPECIMEN DIMENSIONS AND DETAILS

The two specimens were identical in geometry except for the wall thickness. The specimens were 20 ft long (6096 mm), with an outer diameter of 10.60 in (269 mm) and 14.20 in (360 mm) at the tip and butt ends, respectively, which provides an outside taper of 1.5% (0.18 in/ft). The inner diameter for one pole was 5.60 in (142 mm) and 9.20 in (233 mm) for the tip and butt ends, respectively, making a wall thickness of 2.5 in (63.50 mm) along the length of the pole. The inner diameter for the second pole was 6.60 in (167 mm) and 10.20 in (259 mm) for the tip and butt ends, respectively, making a wall thickness of 2.0 in (50.80 mm) along the length of the pole. Although larger size specimens could have been used, the size was chosen to allow for easy transportation from the production plant to the structural laboratory at the University of Alabama at Birmingham. Four layers of CFRP were wrapped around each pole using manufacturer epoxy. The poles were partially wrapped starting at 4.0 ft (1220 mm) from the tip of the pole and extending 12.0 ft (3660 mm) toward the butt of the pole, as shown in Figure 1. For the 2.0 in (50.80 mm) wall thick pole, the first and the third layer of CFRP were wrapped where the carbon fibers oriented parallel to the longitudinal direction of the pole as shown in Figure 2, while the second and the fourth layer were wrapped where the carbon fibers oriented parallel to the circumference of the pole as shown in Figure 1. For the 2.5 in (63.50 mm) wall thick pole, all the layers were wrapped where the carbon fibers were parallel to the circumference of the pole as shown in Figure 1.

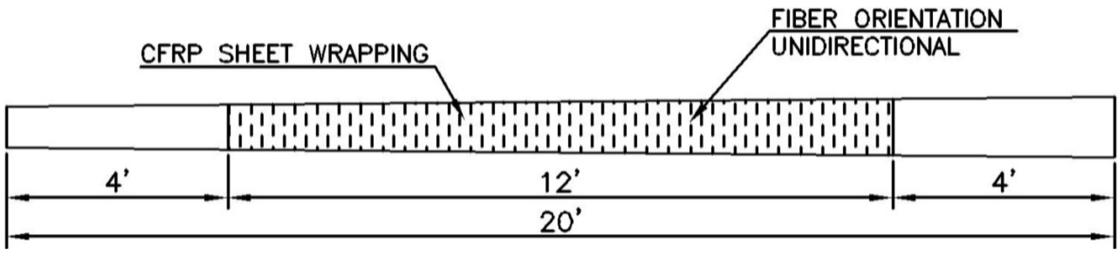

Figure 1. Wrap length and circumferential carbon fiber orientation (specimen P01-2.5-4C)
Note: 1ft = 305 mm

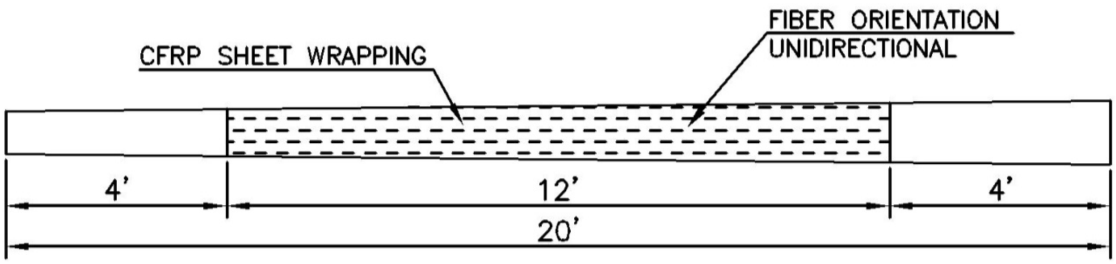

Figure 2. Wrap length and longitudinal carbon fiber orientation (specimen P02-2.0-2C-2L)
Note: 1ft = 305 mm

Table 2 provides a summary of the geometry and details for the test specimens. The first two digits of the specimen ID following the letter “P” represent the pole number, and the number following the first dash represents the wall thickness of the pole. The number preceding the letters “C” and “L” represents the number of CFRP wrapping layers. The letter “C” means that the carbon fibers oriented parallel to the circumference of the pole, whereas the letter “L” means that the carbon fibers oriented parallel to the longitudinal direction of the pole.

Table 2. Specimens dimensions and details

Specimen ID	Conc. Cover (in)	Pole Outer Dia. (in)		Pole Inner Dia. (in)		Pole Length (ft)	Conc. Strength (psi)
		At Tip	At Butt	At Tip	At Butt		
P01-2.5-4C	0.75	10.60	14.20	5.60	9.60	20	11,000
P02-2.0-2C-2L				6.60	10.60		

Note: 1in = 25.4 mm 1ft = 305 mm 1000 psi = 6.89 MPa

TEST SETUP AND PROCEDURE

The pole test specimens were subjected to a four point loading. A schematic diagram of the test setup is shown in Figure 3. The pole specimen rested on two supports. Each support was located 8.0 ft (2440 mm) from center of the pole, forming a distance of 16.0 ft (4880 mm) between the two supports.

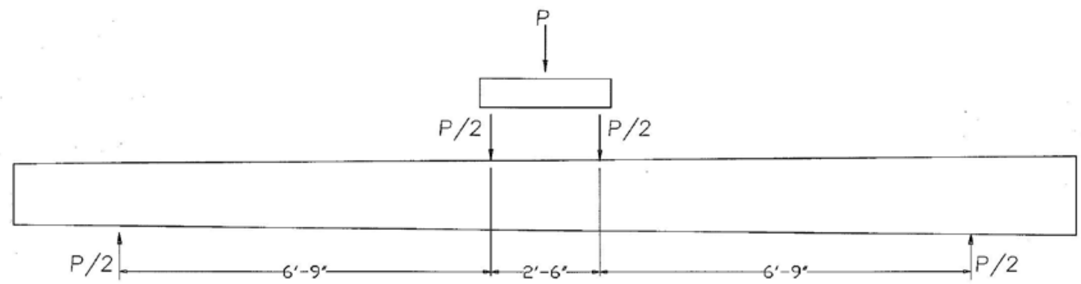

Figure 3. Schematic diagram of test setup
Note: 1in = 25.4 mm 1ft = 305 mm

Two point loads were applied to the pole. Each load was located 1.25 ft (380 mm) from the center of the pole forming a distance of 2.5 ft (760 mm) between the two point loads. Four monotonic loading cycles were applied to each of the specimens with a hydraulic jack. A photograph of test setup is shown in Figure 4.

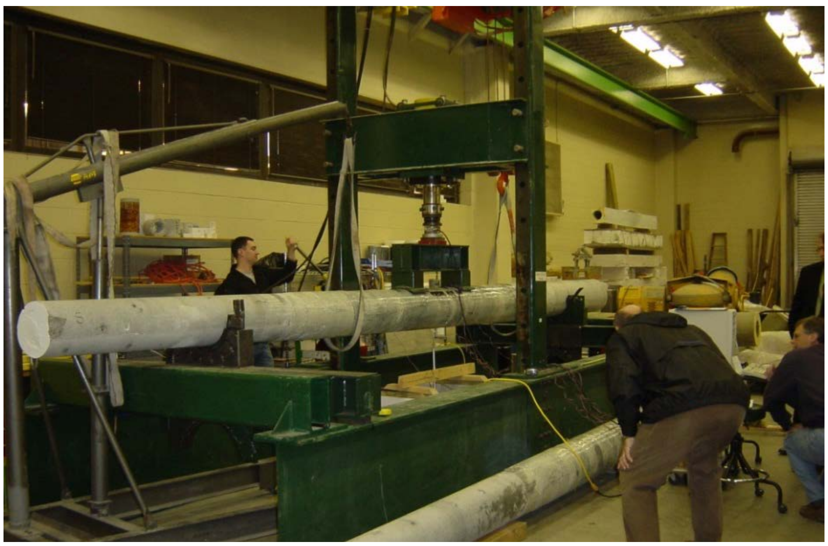

Figure 4. Test setup

Two sets of strain gages were installed. The first set consisted of four strain gages centered along the length of the pole on the top side. Two of the strain gages were located parallel to the circumference of the pole to measure the circumferential strain, and the other two were located parallel to the longitudinal direction of the pole to measure the longitudinal strain. The first set of strain gages is shown in Figure 5.

Figure 5. Location of compression set of strain gages

The second set of strain gages consisted of two strain gages, one under each point load. The strain gages were installed parallel to the longitudinal direction of the pole to measure the longitudinal tensile strain.

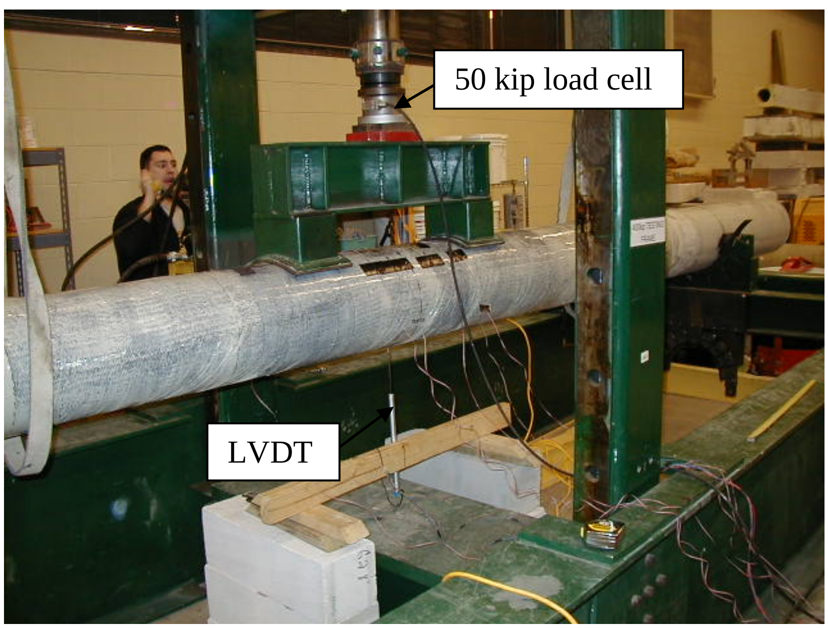

Figure 6. Location of the LVDT and the load cell

The deflection at the center of the pole was measured using Linear Variable Differential Transformers (LVDT), and the load was measured using a 50 kips (220 kN) load cell as shown on Figure 6. The data from the strain gages, deflection and load were transferred to a Data Acquisition System connected to a desktop computer for analysis of data.

TEST RESULTS

The poles were subjected to four load cycles as shown in Table 3. For each load cycle the load was totally released from the pole. The LVDT was removed for safety issues in the third cycle at a load of about 42.0 kips (187 kN) for pole P01-2.5-4C and in the fourth cycle at a load of about 37.0 kips (165 kN) for pole P02-2.0-2C-2L.

A summary of the test results is presented in Table 4. Pole P01-2.5-4C, wrapped in one direction, failed at a higher load and compressive strain than pole P02-2.0-2C-2L, wrapped in two directions. Although the failure load of pole P01-2.5-4C was higher than the failure load of pole P02-2.0-2C-2L by 6%, the compressive strain at failure was higher by 94%. The increase in the failure load is attributed to the difference in the wall thickness of the poles; however, the significant increase in the compressive strain is attributed to the improved confinement provided by the unidirectional wrapping.

Table 3. Load cycles

Specimen ID	Load Cycle			Notes
	Number	From (kips)	To (kips)	
P01-2.5-4C	1	0.0	11.0	Theoretical cracking load
	2	0.0	17.0	60% from the theoretical ultimate load
	3	0.0	43.0	
	4	0.0	44.74	Failure load
P02-2.0-2C-2L	1	0.0	11.0	Theoretical cracking load
	2	0.0	17.0	60% from the theoretical ultimate load
	3	0.0	24.5	90% from the theoretical ultimate load
	4	0.0	42.0	Failure load

Note: 1kip = 4.45 kN

Table 4. Summary of test results

Specimen ID	Failure Load (kips)	Corresponding Moment (ft-k)	Compressive strain at failure
P01-2.5-4C	44.74	151.0	0.0068
P02-2.0-2C-2L	42.21	142.5	0.0035

Note: 1kip = 4.45 kN 1ft-k = 1.35 kN-m

Deflection

Figure 7 shows the load deflection curves of the two specimens from zero loading up to failure. The poles were deflecting linearly with load up to approximately 14.5 kips (64.5 kN); above this load, the poles were deflecting non-linearly with load up to failure. It can also be seen that in the nonlinear zone, pole P01-2.5-4C, wrapped in one direction, provided higher deflection values (for the same load) than pole P02-2.0-2C-2L, wrapped in two directions. This indicates that wrapping the pole in one direction increased the ductility of the member.

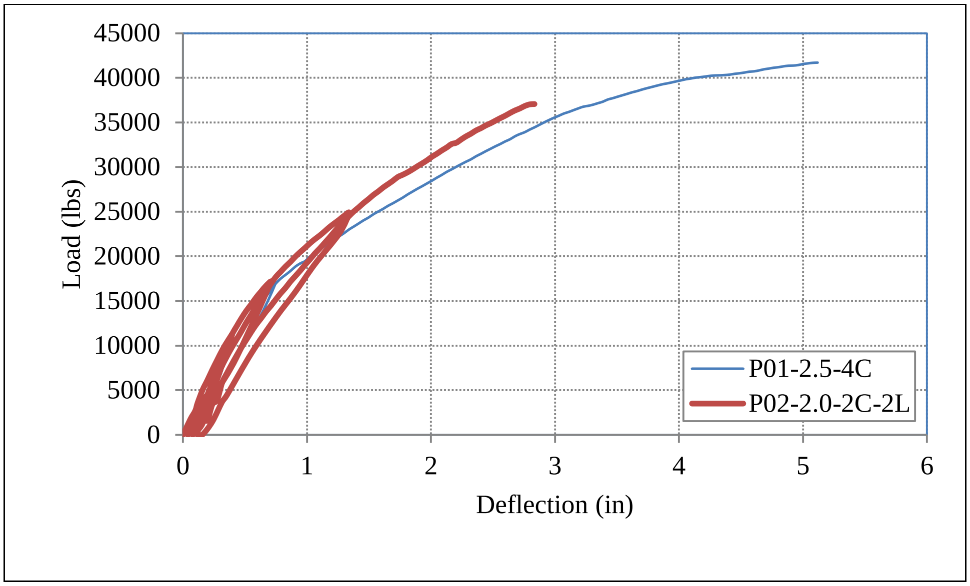

Figure 7. Load-deflection curve for the specimens
Note: 1in = 25.4 mm 1lbs = 4.45 N

Taking a closer look at the curves, Figure 8 provides a plot of the load deflection curves from zero load up to a load of 11.0 kips (49 kN), which is considered the theoretical cracking load of the specimens and represents the end of their first loading cycle. The two specimens deflected linearly with load and had almost the same deflection values. It can also be seen that the residual deflection after unloading the specimens did not exceed 0.04 in (1.0 mm).

Figure 9 provides a plot of the load deflection from zero load up to a load of about 17.0 kips (75.6 kN), which represents the end of the second load cycle. The two specimens deflected linearly with load and had almost the same deflection values up to a load of about 14.5 kips (64.5 kN), after which the two curves started to deviate from each other. Deviation of the curves indicates the formation of cracks, meaning that the cracking load of the specimens was about 14.5 kips (64.5 kN). This value is higher than the theoretical value by about 30%. It can also be noticed that the residual deflection after unloading the specimens did not exceed 0.08 in (2.0 mm).

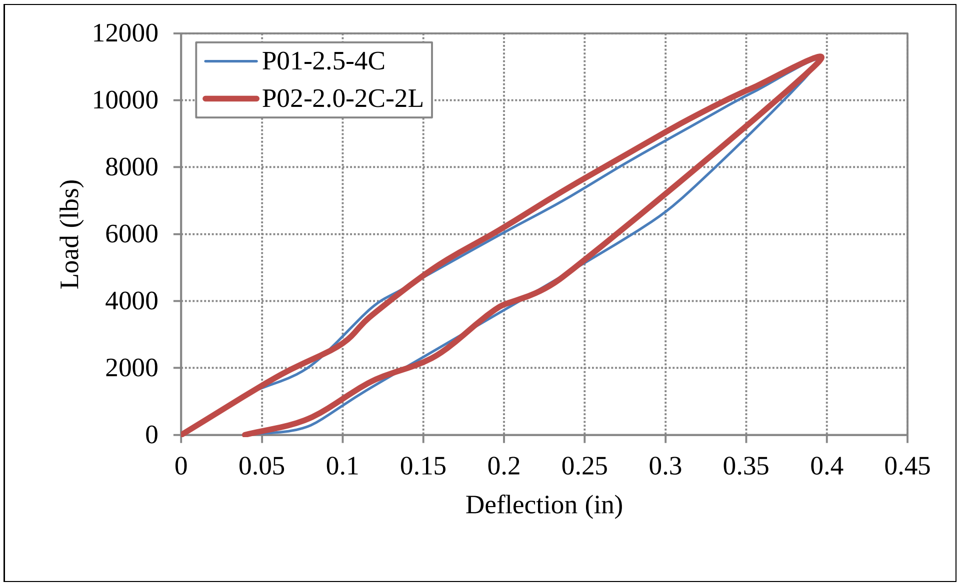

Figure 8. Load-deflection curve up to a load of 11.0 kips
Note: 1in = 25.4 mm 1lbs = 4.45 N

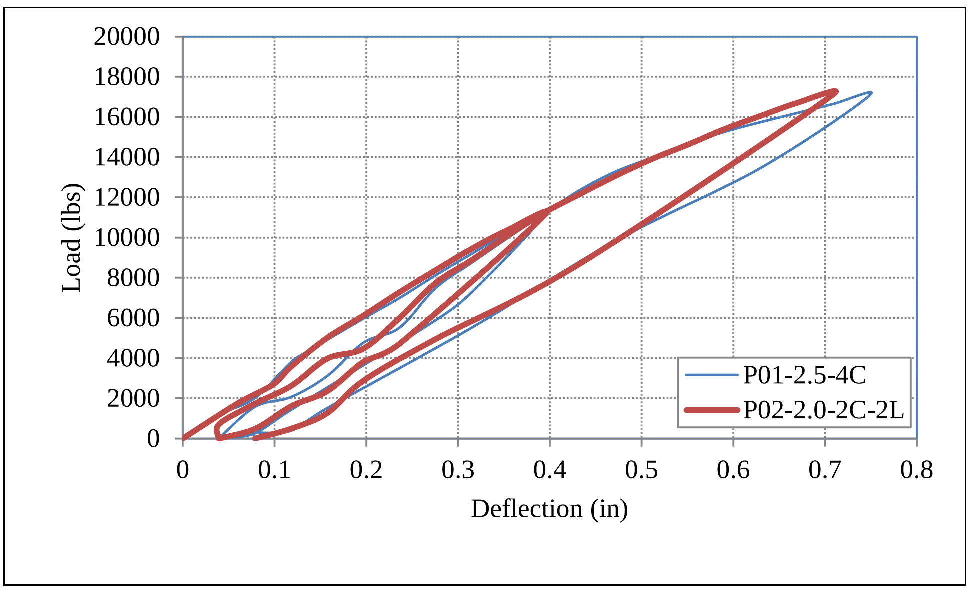

Figure 9. Load-deflection curve up to a load of 17.0 kips
Note: 1in = 25.4 mm 1lbs = 4.45 N

Strain Gages

Figure 10 shows the load versus strain of the first set of strain gages for the two poles. Positive strains are the tensile circumferential strain, whereas the negative strains are the compressive longitudinal strains. It can be seen from Figure 10 that there was no significant difference in the tensile circumferential strains of the two poles up to a load of 35 kips (159.0 kN). It is also evident that the slope of the tensile circumferential strains is larger than the slope of the compressive longitudinal strains and there is no significant difference in the compressive longitudinal strains of the two poles up to a load of 25 kips (11.35 kN). Moreover, at lower loads, the tensile circumferential strain was about 20% of the compressive longitudinal strain; however, at failure, the tensile circumferential strain was about 50% of the compressive longitudinal strain for the two poles. At failure of pole P01-2.5-4C, wrapped in one direction, the maximum compressive longitudinal strain was 0.0068 and the maximum tensile circumferential strain was 0.0036, while at failure of pole P02-2.0-2C-2L, wrapped in two directions, the maximum compressive longitudinal strain was 0.0035 and the maximum tensile circumferential strain was 0.0018. Although there was a significant difference in the failure strain of the two poles, the ratio between the tensile circumferential strain and the compressive longitudinal strain remained constant.

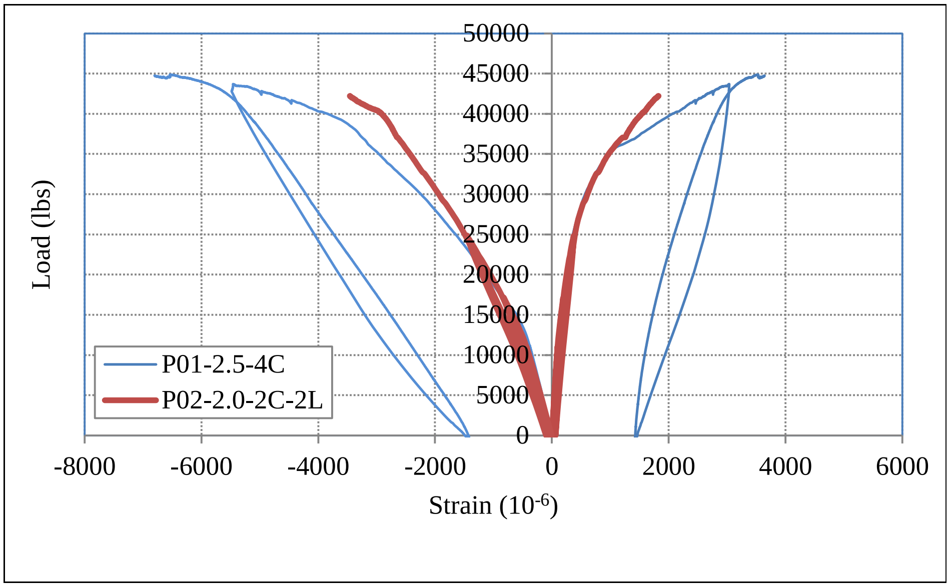

Figure 10. Load versus strain for the tested poles
Note: 1lbs = 4.45 N

Failure Mode

Two types of failure modes were observed. For pole P01-2.5-4C, wrapped in one direction, the pole failed in combined flexure and shear right outside the loading point toward the butt end of the pole. The pole failure is shown in Figure 11. For pole P02-2.0-2C-2L, wrapped in two directions, the pole failed in compression just next to the left load point toward the tip end of the pole. At failure the concrete crushed explosively in compression as shown in Figure 12. Moreover, significant deflection before failure was observed for pole P01-2.5-4C, wrapped in one direction, compared to pole P02-2.0-2C-2L, wrapped in two directions, as shown in Figure 13.

Figure 11. Failure mode of pole P01-2.5-4C, wrapped in one direction

Figure 12. Failure mode of pole P02-2.0-2C-2L, wrapped in two directions

Figure 13. Deflection of pole P01-2.5-4C, wrapped in one direction, just before failure

Failure load

Figure 14 shows the experimental failure load of the specimens compared to the theoretically calculated values. It can be seen that wrapping increased the ultimate load capacity of the poles by about 35% compared to the theoretical values.

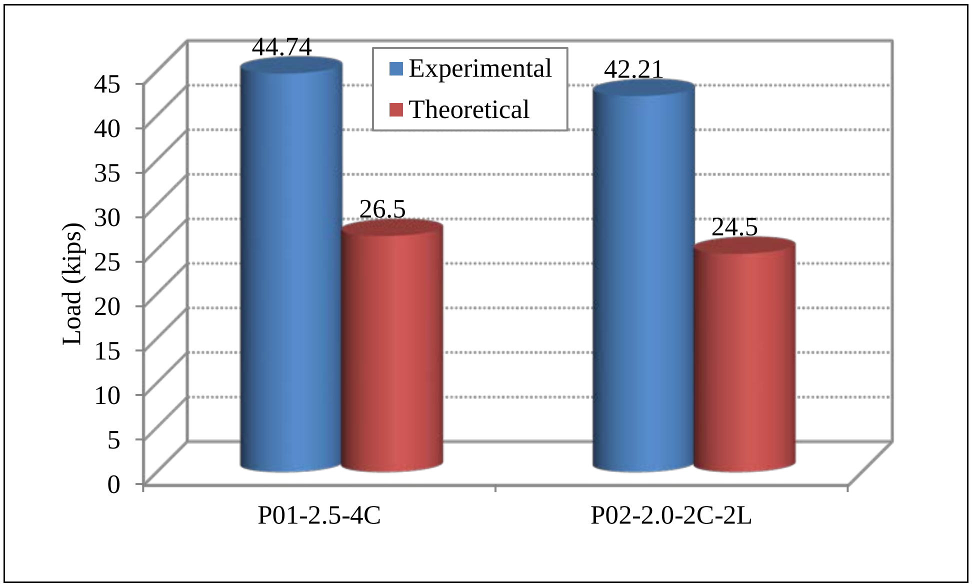

Figure 14. Experimental versus theoretical failure loads
Note: 1kips = 4.45 kN

CONCLUSIONS

Strengthening of prestressed spun concrete poles using CFRP wrapping was studied in this paper. The poles were wrapped using CFRP laminates and then subjected to a four point monotonic loading test. The conclusions of this study can be summarized as follows:

1. Strengthening prestressed spun concrete poles using CFRP wrapping is a successful technique to increase the ultimate capacity of the poles.
2. CFRP wrapping increased the ultimate capacity of the poles by about 35% compared to the theoretical values.
3. Unidirectional wrapping provided better confinement to the poles than bidirectional wrapping. The failure strain of the pole wrapped in one direction was 94% higher than the failure strain of the pole wrapped in two directions.
4. Unidirectional wrapping increased the ductility of the pole compared to bidirectional wrapping. The pole wrapped in one direction provided significant amount of deflection prior to failure as compared to the pole wrapped in two directions.
5. Wrapping direction has no significant effect on the ultimate capacity of the pole. There was no significant difference in the ultimate capacity of the poles wrapped in one and in two directions (only 6% difference).
6. CFRP unidirectional wrapping is recommended for strengthening prestressed spun concrete poles due to the added confinement it provides.
7. Additional tests with different number of CFRP layers and orientation schemes will provide more information about strengthening prestressed spun concrete poles with CFRP wrapping, including more data that will allow to develop equations calculating the ultimate capacity of prestressed spun concrete poles strengthened with CFRP wrapping.

ACKNOWLEDGEMENTS

The authors acknowledge Valmont-Newmark for their financial support in producing the test samples and providing the repair and strengthening materials.

REFERENCES

1. ACI 440.2R-08. (2008). “Guide for the Design and Construction of Externally Bonded FRP Systems for Strengthening Concrete Structures.” Prepared by the ACI committee 440.
2. Yazici, V., and Hadi, M. (2009). “Axial Load-Bending Moment Diagrams of Carbon FRP Wrapped Hollow Core Reinforced Concrete Columns” ASCE, Journal of Composites for Construction, Vol. 13, No. 4, pp. 262-268.
3. Durham, S. A., Heymsfield, E., and Jones, J. X. (2009). “Retrofitting Precast Bridge Beams with Carbon Fiber Reinforced Polymer Strips for Shear Capacity”, ASCE, Journal of Performance of Constructed Facilities, Vol. 23, No. 4, pp. 219-226.

4. Brena, S. F., Bramblett, R. M., Wood, S. K., and Kreger, M. E. (2003). "Increasing Flexural Capacity of Reinforced Concrete Beams Using Carbon Fiber Reinforced Polymer Composite." ACI Structural Journal, Vol. 100, No. 1, pp. 36-46.
5. Shalaby, A., Fouad, H. F., and Albanese, R. (2008). "Flexural Behavior of Spun Concrete Poles Reinforced with CFRP Bars." Proceedings of the 54th PCI Annual Convention, Oct. 4-7, 2008, Orlando, Florida.
6. ACI 440.1R-06, (2006), "Guide for the Design and Construction of Structural Concrete Reinforced with FRP Bars." Prepared by the ACI committee 440.
7. Toutanji, H. A., and Saafi, M. (2000). "Flexural Behavior of Concrete Beams Reinforced with Glass Fiber-Reinforced Polymer (GFRP) bars." ACI Structural Journal, Vol. 97, No. 5, pp. 712-719.
8. Benmokrane, B., Chaallal, O., and Masmoudi, R. (1996). "Flexural Response of Concrete Beams Reinforced with FRP Reinforcing Bars." ACI Structural Journal, Vol. 93, No. 1, pp. 46-55.
9. Chahrour, A. H. and Soudki, K. A. (2006). "Structural Retrofitting of Deteriorated Concrete Lighting Poles Using FRP Sheets in Wet Layup- Field Application." ASCE, Journal of Composites for Construction, Vol. 10, No.3, June 1, 2006, pp. 234-243.
10. Sause, R., Harries, K. A., Walkup, S. L., Pessiki, S. and Ricles, J. M. (2004). "Flexural Behavior of Concrete Columns Retrofitted with Carbon Fiber Reinforced Polymer Jackets." ACI Structural Journal, Vol. 101, No. 5, pp. 708-716.
11. Pessiki, S., Harries, K. A., Sause, R., Ricles, J. M. (2001). "Axial Behavior of Reinforced Concrete Columns Confined with FRP Jackets." ASCE, Journal of Composites for Construction, Vol. 5, No. 4, pp. 237-245.
12. Debaiky, A., Green, M., and Hope, B. (2006). "Long-Term Monitoring of CFRP Wrapped Reinforced Concrete Columns Under Severe Environment." ACI Structural Journal, Vol. 103, No. 6, pp. 226-234.
13. Seible, F., Priestley, M. J. N., Hegemier, G. A., and Innamorato, D. (1997). "Seismic Retrofit of RC Columns with Continuous Carbon Fiber Jacket." ASCE, Journal of Composites for Construction, Vol. 1, No. 2, pp. 52-62.
14. ASTM Standard A82. (2007). "Standard Specification for Steel Wire, Plain, for Concrete Reinforcement" ASTM International, West Conshohocken, PA, www.astm.org.
15. ASTM Standard A416. (2006). "Standard Specification for Steel Strand, Uncoated Seven-Wire for Prestressed Concrete" ASTM International, West Conshohocken, PA, www.astm.org.